Biochimica et Biophysica Acta 1838 (2014) 2635–2645

Contents lists available at ScienceDirect

Biochimica et Biophysica Acta

journal homepage: www.elsevier.com/locate/bbamem

The role of sterols in the lipid vesicle response induced by the pore-forming agent nystatin

Luka Kristanc [a,*], Bojan Božič [a,b], Gregor Gomišček [a,c]

[a] Institute of Biophysics, Faculty of Medicine, University of Ljubljana, Ljubljana, Slovenia
[b] Jožef Stefan Institute, Ljubljana, Slovenia
[c] Faculty of Health Sciences, University of Ljubljana, Ljubljana, Slovenia

ARTICLE INFO

Article history:
Received 22 January 2014
Received in revised form 3 May 2014
Accepted 16 May 2014
Available online 24 May 2014

Keywords:
Nystatin
Giant phospholipid vesicle
Transmembrane pore
Sterol
Tension-pore formation

ABSTRACT

The influences of ergosterol and cholesterol on the activity of the nystatin were investigated experimentally in a POPC model membrane as well as theoretically. The behavior of giant unilamellar vesicles (GUVs) under osmotic stress due to the formation of transmembrane pores was observed on single vesicles at different nystatin concentrations using phase-contrast microscopy. A significant shift of the typical vesicle behavior, i.e., morphological alterations, membrane bursts, slow vesicle ruptures and explosions, towards lower nystatin concentrations was detected in the ergosterol-containing vesicles and a slight shift towards higher nystatin concentrations was detected in the cholesterol-containing membranes. In addition, the nystatin activity was shown to be significantly affected by the ergosterol membrane's molar fraction in a non-proportional manner. The observed tension-pore behavior was interpreted using a theoretical model based on the osmotic phenomena induced by the occurrence of size-selective nystatin pores. The number of nystatin pores for different vesicle behavior was theoretically determined and the role of the different mechanical characteristics of the membrane, i.e., the membrane's expansivity and bending moduli, the line tension and the lysis tension, in the tension-pore formation process was quantified. The sterol-induced changes could not be explained adequately on the basis of the different mechanical characteristics, and were therefore interpreted mainly by the direct influences of the membrane sterols on the membrane binding, the partition and the pore-formation process of nystatin.

1. Introduction

Nystatin is an antimicotic agent that belongs to polyene macrolid antibiotics, a family of compounds characterized by a large lactone ring with three to eight conjugated double bonds. It has a broad spectrum of activity against fungi, but it is mainly used for the topical treatment of mucosal and cutaneous *Candida* infections due to its toxic effects when administered systemically [1,2]. As a pore-forming agent, nystatin could also be capable of translocating different cargo molecules into the cells, which makes it a potential specific drug-delivery agent. The biological activity of the polyenes seems to result from their ability to form barrel-like, membrane-spanning channels in the plasma membrane of antibiotic-sensitive organisms [3–5]. These transmembrane pores have size-selective properties: in the case of nystatin they are only permeable to solutes no larger than glucose [6]. The increase in the plasma-membrane permeability to ions and small molecules causes a disturbance to the cellular electrochemical gradients, which ultimately leads to cell lysis and death [3].

Like many cellular membrane activities [7–9] the polyene mode of action has been shown to be affected by the sterol composition in the membrane [10–12]. These effects are probably associated with the sterol-induced changes in the membrane's structural and dynamic properties, such as the regularity of the membrane's lipid organization, the membrane's free volume and the motility of the membrane's constituents [8–12]. Several studies have reported the tendency of cholesterol to increase the line tension and the membrane-expansivity modulus of lipid membranes [13–19]. The addition of ergosterol into the membranes also results in an increase of the membrane-expansivity modulus and the vesicle lysis tension; however, these membrane-stabilizing effects are smaller than those of cholesterol [20–22]. Additionally, various conceptual models were designed to explain the nature of the sterol-lipid membrane interactions [23–25]. The superlattice models suggest distributions with local maxima at theoretically predictable sterol critical molar fractions [26–28].

A significant impact of sterols on the nystatin mode of action has been shown by studies undertaken, in particular, with cholesterol- and ergosterol-containing membranes [29–31]. Many different molecular mechanisms describing the role of sterols in the pore-formation

* Corresponding author at: Institute of Biophysics, Faculty of Medicine, University of Ljubljana, Vrazov trg 2, 1000 Ljubljana, Slovenia. Tel.: +386 1 5437600, +386 40 566 950 (mobile); fax: +386 1 5437601.
E-mail address: luka.kristanc@gmail.com (L. Kristanc).

http://dx.doi.org/10.1016/j.bbamem.2014.05.019
0005-2736/

process have been presented, including the formation of specific antibiotic-sterol complexes [32,33] and the influences on the polyene membrane's partition due to the sterol-induced changes in the membrane's lipid organization [34,35]. The studies revealed that the increased regularity of the membrane's lipid organization by the addition of cholesterol inhibits the partition of polyenes into the membrane [11–13]. Ergosterol has an even more pronounced lipid-ordering effect than cholesterol in the bilayers formed with saturated lipids [36–39]; however, these effects are substantially diminished in the case of the membranes consisting of an unsaturated lipid like POPC [39]. This is in accordance with the facilitating influences of ergosterol on the nystatin activity in POPC membranes [40]. Furthermore, it has been shown that nystatin has a tendency to form intra-membrane complexes with ergosterol, which could be a major contributing factor to the increase in the nystatin pore-forming activity [32,33]. The changed fluorescence lifetimes of nystatin indicate the formation of nystatin-nystatin or nystatin-sterol complexes [41]. In addition, it has also been found that polyenes are able to form pores in membranes that do not contain any sterols [29,42,43]. The number of nystatin molecules forming the transmembrane pore is estimated to be between 4 and 12 [5,44], and the measured effective radii are mostly in the range between 0.4 and 0.5 nm [45,46]. The radius of nystatin pores was not found to be influenced by the addition of cholesterol or ergosterol into the membrane [47].

Further theoretical and experimental studies are needed to elucidate the polyene-membrane interaction and to obtain a more precise and comprehensive understanding of the influences of the variations in the membrane's sterol content. Our recent work with sterol-free giant unilamellar vesicles (GUVs) and nystatin has revealed some distinct vesicle behavior patterns [43] that could not be obtained from studies on the bulk properties of the membrane-nystatin interactions for small and large unilamellar vesicles [5,30,31]. The GUVs were chosen because they can be manipulated and observed individually, using a micropipette manipulation technique and a phase-contrast microscopy. Hence, we also apply our approach in the present study, in which we observe the influences of membrane sterols (with a focus on ergosterol and its molar fraction) on the nystatin membrane activity and establish a comparison of the behavior of sterol-free and sterol-containing GUVs. We relate the experimental results to the predictions of the theoretical model based on the osmotic phenomena induced by the occurrence of size-selective nystatin pores. Our primary concern is an understanding of the observed differences in the vesicle behavior in connection with the effects of sterols on the membrane's mechanical properties as well as on the formation of nystatin pores. We discuss the results in the context of the tension-pore formation process and the findings in the literature.

2. Materials and methods

2.1. Preparation of vesicles (GUVs) and nystatin solutions

The GUVs were prepared from POPC and/or POPC-sterol mixtures according to the modified method of Angelova et al. [48]. The ergosterol (Sigma-Aldrich, USA) was added to the POPC (Avanti Polar Lipids, USA) in molar fractions of 15, 30 or 45% and the cholesterol (Avanti Polar Lipids, USA) in a 45% molar fraction. The POPC and/or the POPC-sterol mixtures were dissolved in a 1:1 chloroform-methanol solution, spread over platinum electrodes and vacuum dried. Afterwards, the electrodes were placed in an electroformation chamber filled with 2 ml of 0.2-mol/l sucrose solution. An AC electric field was applied, which was stepwise reduced from a starting value of 1 V/mm and 10 Hz to a final value of 0.1 V/mm and 1 Hz. The formed vesicles containing the sucrose solution were transferred in an isomolar glucose solution and kept there at room temperature. The samples were used within three days of preparation; however, the sterol-containing vesicles were not used earlier than two days after their preparation in order to enable a sufficient level of sterol lateral distribution in the membranes.

A stock suspension of 10 mmol/l nystatin was prepared from the lyophilized nystatin (Fluka, Sigma, USA). Pure methanol was used as a solvent, since nystatin has poor water solubility. It was stored in a dark place at −4 °C. The nystatin solutions with the desired concentrations were prepared immediately prior to the experiment. A stock suspension of the appropriate volume was diluted with a 0.2-mol/l glucose solution and stirred using a vortex. The methanol was maintained at volume fractions under 10% in order to minimize its effects on the phospholipid membrane; the methanol volume fraction only increased by 1% as the nystatin concentration was increased by 100 μmol/l. It should be noted, as an experimental limitation, that the saturation effects of nystatin in the surrounding solution associated with its poor water solubility were detected at nystatin concentrations higher than 600 μmol/l.

2.2. Experimental set-up and procedure

The GUVs were observed with an inverted microscope (IMT-2, Olympus, Japan; objective LWD CDPlan40X, NA = 0.55) using phase-contrast microscopy. The images were continuously acquired with a chilled black-and-white CCD camera (C5985, Hamamatsu, Japan) and stored in a personal computer. The images of the vesicles were kept focused in the equatorial plane during the experimental procedure.

A two-compartment cell was used for the vesicle manipulation [43]. The first compartment was filled with the glucose solution that contained the vesicles. The vesicles with an appropriate size and with no anomalies were selected and transferred into the second, measuring compartment using a micropipette manipulation system. The measuring compartment was filled with nystatin solutions of the desired concentrations. The glucose concentrations were equal to 0.2 mol/l in both the compartments. The nystatin concentration remained practically constant during the transfer due to the much smaller volume of the transferred solution compared to the volume of the measuring compartment. The measurements were performed at a room temperature of 24 ± 1 °C.

Individual unilamellar, nearly spherical vesicles with diameters of 40 ± 20 μm were chosen and transferred in groups of 1–5 vesicles into the measuring compartment with nystatin concentrations of between 10 and 800 μmol/l. The vesicles were observed within the first 60 min after their transfer, depending on the duration of the investigated process. At the beginning of each measuring sequence, the control experiments were performed in an isomolar glucose solution without nystatin in order to test the stability of the prepared GUVs and the influence of the micromanipulation procedure. In addition, the GUVs were exposed to a methanol-glucose solution without nystatin in order to check the influence of methanol. The methanol volume fraction was 6% that is our maximal methanol concentration used in experiments with nystatin.

2.3. Image analysis

The images were evaluated qualitatively and quantitatively [43]. Qualitatively, the characteristic vesicle behavior patterns were determined at different nystatin concentrations based on a continuous observation of the phase-contrast images. Quantitatively, the images were assessed in terms of the brightness profile along the line across the vesicle membrane in a radial direction, which was fitted in the halo region by a Gaussian curve [49]. The halo intensity was determined at discrete time intervals and used as a measure of the changing sucrose-glucose ratio inside the vesicle. All the images were analyzed using in-house-produced software, while the quantitative results were evaluated using standard statistical procedures.

3. Experimental results

3.1. Characteristic behavior of the GUVs at low nystatin concentrations

At low nystatin concentrations, i.e., at concentrations below approximately 100 μmol/l, no significant changes in the sterol-free vesicle behavior compared to the control experiments were detected [43]. Similarly, the cholesterol-containing GUVs demonstrated no significant morphological alterations or any halo-intensity decrease over the whole measuring period of one hour in this nystatin concentration range (Figs. 1a and 2). Furthermore, the transfer of vesicles into glucose-methanol solution without nystatin did not cause any significant vesicle fading in sterol-free (Fig. 2) and sterol-containing GUVs.

In contrast, the ergosterol-containing GUVs demonstrated various shape transformations as well as different osmotic phenomena following a short, post-transfer incubation period of a few minutes. At the lowest measured nystatin concentrations (around 10 μmol/l) diverse membrane formations were observed, whereas the halo intensity of the GUVs was not reduced significantly. The shapes and sizes of membrane formations were quite diverse, ranging from filamentous protrusions to necklace-shaped rows or groups of spheres. The most commonly observed formations were external protrusions, slowly growing over time. The described formations were similar to those observed in cholesterol-containing vesicles at significantly higher concentrations (Fig. 1b).

However, the effects of ergosterol molar fraction became apparent at nystatin concentrations equal to or greater than 25 μmol/l. The vesicles containing 30 mol% of ergosterol experienced a slow and partial fading at 25-, 50- and 75-μmol/l nystatin concentrations (Fig. 2). Their halo intensities decreased to 69%, 61% and 57% of the initial values in the measuring period of one hour with an average halo-intensity decrease rate equal to $(1.05 \pm 0.15) \times 10^{-4}\,s^{-1}$. The slow ruptures of the vesicles were detected at a minimum nystatin concentration of 100 μmol/l for this ergosterol fraction (Fig. 2). The term slow rupture denotes a large membrane opening, lasting up to several seconds, which is accompanied by a substantial leak of the vesicle content and results in a significant loss of its halo intensity (Fig. 3a; see also Appendix B). The membrane reseals afterwards. This cycle of membrane opening and resealing is repeated several times. More seldom, a stable opening with a distinctive orifice is observed around which an amorphous relict of the vesicle is formed [43]. At the end, the vesicle disintegrates into amorphous lipid debris (Fig. 3a). On the other hand, the nystatin effects were much more intense at 15 and 45 ergosterol mol% – slow ruptures of the vesicles were observed already for a 25-μmol/l nystatin concentration. Survival times, defined as the times from the vesicle transfer into the nystatin solution to the beginning of the vesicle rupture, were 1363 s and 712 s for the vesicles containing 15 and 45 mol% ergosterol at a 25-μmol/l nystatin concentration. These survival times were significantly shorter than the survival times of the vesicles containing 30 mol% of ergosterol at a 100-μmol/l nystatin concentration, the average value of which was 1932 s (Fig. 2).

Thus, the observations show that a change in the ergosterol molar fraction of 15 mol% induced a dramatic change in the vesicle response at a 25-μmol/l nystatin concentration. Namely, an ergosterol content

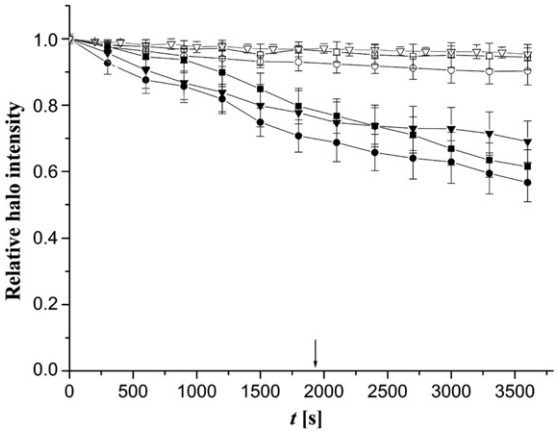

Fig. 2. Three characteristic responses of sterol-free and sterol-containing GUVs at low nystatin concentrations (up to 100 μmol/l). Insignificant fading of the GUVs without sterols (□, n = 9) and the GUVs containing 45 mol% cholesterol (○, n = 16) at a 100-μmol/l nystatin concentration. Significant (partial) fading of the GUVs containing 30 mol% ergosterol at 25 μmol/l (▼, n = 7), 50 μmol/l (■, n = 10) and 75 μmol/l (●, n = 8) nystatin concentration. Slow ruptures of GUVs containing 30 mol% ergosterol at a 100-μmol/l nystatin concentration (n = 8) with an average survival time equal to 1930 s are depicted by a vertical arrow. No significant fading of sterol-free GUVs was observed in a control, 6% methanol concentration without nystatin (▽, n = 9). The halo-intensity values are normalized with respect to the initial halo-intensity value of the individual vesicles; vertical bars represent standard deviations.

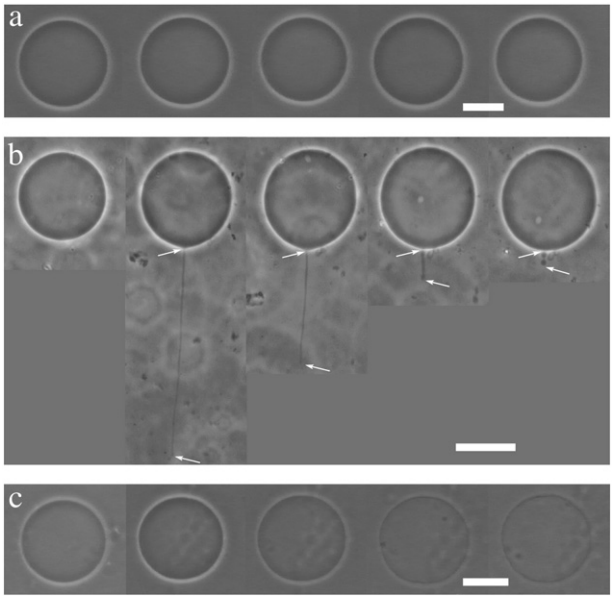

Fig. 1. Characteristic behavior patterns of 45-mol% cholesterol-containing vesicles: a) Normal behavior of the GUVs at a nystatin concentration of 100 μmol/l. The snapshots were taken in 10-minute intervals. b) The occurrence of various membrane formations at a nystatin concentration of 200 μmol/l. The arrows indicate the beginning and the end of the protrusion, gradually evolving from predominantly thin tethers to spherically shaped necklaces. Note the absence of these structures on the first image. The snapshots were taken at 6, 17, 21, 25 and 29 min after the transfer into the nystatin solution. c) An almost complete loss of halo intensity as a consequence of many transient membrane bursts at 300 μmol/l nystatin concentration. The snapshots were taken at 1, 6, 27.5, 39.5 and 48 min after the transfer into the nystatin solution. The scale bars indicate a length of 20 μm.

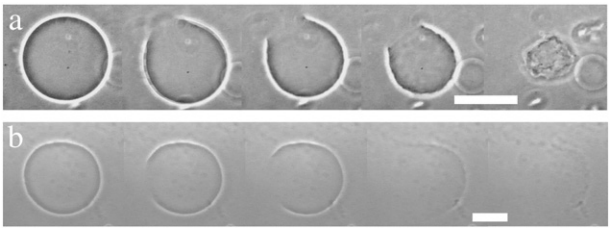

Fig. 3. Different types of vesicle ruptures (see also text and Appendix B for more detailed descriptions): a) A typical slow rupture of the vesicle. The snapshots were taken approx. 21 min after the transfer of the 30-mol% ergosterol-containing vesicle into the 200-μmol/l nystatin solution. The duration of the slow rupture was approximately 2 s. b) A typical fast rupture (explosion) of the vesicle. The first snapshot was taken approx. 4.5 min after the transfer of the 45-mol% ergosterol-containing vesicle into a 500-μmol/l nystatin solution. The next consecutive snapshots were taken 0.07, 0.2, 0.33 and 0.5 s after the first one. The scale bars indicate a length of 20 μm.

decrease from 30 to 15 mol%, or its increase from 30 to 45 mol%, led to a change in the characteristic vesicle behavior from membrane bursts to slow ruptures (Fig. 2).

3.2. Characteristic behavior of GUVs at intermediate nystatin concentrations

The behavior of sterol-free vesicles in an intermediate nystatin concentration range, i.e., between 100 and 400 μmol/l, was characterized in terms of various membrane formations for the lower region of these concentrations and an almost complete loss of halo intensity as a consequence of many transient membrane bursts for the higher region of these concentrations. Slow ruptures of the vesicles were only characteristic for nystatin concentrations around 400 μmol/l. On the other hand, the behavior patterns of the sterol-containing vesicles were found to be, as already seen for the low nystatin concentration range, strongly dependent on the membrane's sterol composition.

Vesicle membrane formations and fading were observed in the experiments with 45 mol% cholesterol-containing vesicles in this nystatin concentration range. Their fading was slow and partial at a 200-μmol/l nystatin concentration, and it was often accompanied by membrane formations of different shapes (Fig. 1b). Substantially higher rates of halo-intensity decrease and almost complete losses of halo intensity, without shape changes, were measured after approximately 45 and 25 min for 300- and 400-μmol/l nystatin concentrations (Fig. 4, Table 1). A series of transient membrane bursts connected with the loss of vesicle content could be observed (Fig. 1c). During each burst, the vesicle membrane opens transiently and a minor fraction of the vesicle content is extruded out of the vesicle. The cycle of membrane opening and resealing is repeated without the destruction of the vesicle [43].

A comparison with the sterol-free vesicles depicts a comparable fading for 200-μmol/l nystatin; however, the effect of the addition of cholesterol into the membrane could clearly be seen at 300- and 400-μmol/l nystatin concentrations (Fig. 4, Table 1). Significantly lower halo-intensity decrease rates were found in the cholesterol-containing GUVs. Note that this rate was lower even for the 100-μmol/l higher nystatin concentration in cholesterol-containing vesicles, i.e., at 400 μmol/l, if compared to the sterol-free GUVs at the 300-μmol/l nystatin concentration (Fig. 4, Table 1). The influence of cholesterol content becomes even clearer if the characteristic behavior pattern of the cholesterol-containing vesicles and the sterol-free ones are compared at the same, 400-μmol/l nystatin concentration. It should be pointed out that the cholesterol-containing vesicles are still in the regime of transient bursts, while the sterol-free ones already experience slow ruptures at this nystatin concentration.

In contrast, the ergosterol-containing GUVs already demonstrated slow and fast ruptures over the entire intermediate nystatin concentration range (Fig. 4). As their name implies, fast ruptures or explosions indicate a more sudden event than slow ruptures. Typically, a quick disintegration of the entire vesicle is observed, often proceeded by a discrete bulge at the site of the breaking membrane (Fig. 3b; see also Appendix B). During the explosion, the vesicle membrane suddenly opens and the vesicle, which seemed intact just a fraction of a second ago, simply disappears, leaving almost no visible traces behind. The average vesicle survival times differed significantly with respect to the membrane's ergosterol content. They were the shortest for the 45 mol% and the longest for the 30 mol% ergosterol-containing GUVs with their values equal to 386 s and 1114 s for the 200-μmol/l nystatin concentration, while the average survival time for the 15-mol%-containing GUVs was in the middle, with its value of approximately 650 s.

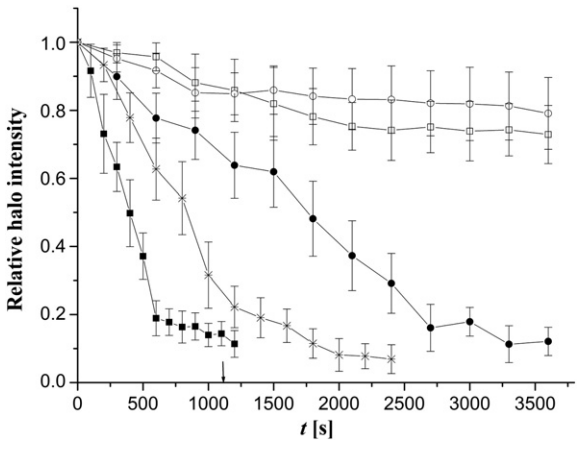

Fig. 4. Typical responses of sterol-free and sterol-containing GUVs at intermediate nystatin concentrations. Partial fading of the GUVs without sterols (□, n = 7) and the GUVs containing 45 mol% cholesterol (○, n = 11) at 200 μmol/l. Almost total fading of the GUVs without sterols (■, n = 8) and the GUVs containing 45 mol% cholesterol at 300 μmol/l (●, n = 10) and at 400 μmol/l (·, n = 8). The average survival time of the slow ruptures of GUVs containing 30 mol% ergosterol at a 200-μmol/l nystatin concentration (n = 9) is depicted by a vertical arrow. The halo-intensity values are normalized with respect to the initial halo-intensity value of the individual vesicles; vertical bars represent standard deviations.

3.3. Characteristic behavior of GUVs at high nystatin concentrations: the dependence of vesicle ruptures on the membrane composition and nystatin concentration

At nystatin concentrations higher than 400 μmol/l, vesicle ruptures were observed to substitute for the fading process of the vesicles, which took place due to the membrane bursts (transient pores), also in the cholesterol-containing and sterol-free membranes. The concentration threshold for the appearance of vesicle ruptures was found to be at 500 μmol/l for the 45-mol% cholesterol-containing GUVs and at a 400-μmol/l nystatin concentration for the sterol-free GUVs, both of which are substantially higher than the ergosterol-containing GUVs (Figs. 4 and 5). To recall, the 30-mol% ergosterol-containing GUVs demonstrated a tendency to rupture even at 100 μmol/l, while the 15- and 45-mol% ergosterol-containing GUVs started to rupture at nystatin concentrations even as low as 25 μmol/l (Figs. 2, 4 and 5).

The fractions of slow ruptures at different nystatin concentrations and vesicle compositions are shown in Fig. 5. The incidence of slow ruptures was found to decrease with increasing nystatin concentrations for all the measured vesicle compositions. Slow ruptures were the predominant type of vesicle ruptures for concentrations up to 500 μmol/l; moreover, fast ruptures (explosions) were very rarely encountered at nystatin concentrations below 100 μmol/l. In addition, slow ruptures were more frequently observed for the 30-mol% ergosterol-containing GUVs than for the 15- and 45-mol% ergosterol-containing GUVs in the nystatin concentration range between 100 and 500 μmol/l (Fig. 5). However, a significant shift towards the explosions occurred at nystatin concentrations around 550 μmol/l, and this type of rupture became the predominant one (Fig. 5). A shift between these two types of ruptures occurred in a relatively narrow concentration range of approximately 100 μmol/l for all the vesicle compositions. However, it appeared to be much less abrupt and less significant for the cholesterol- and ergosterol-containing GUVs in comparison to that observed for the sterol-free ones. The nystatin concentration span characterized by the predominance of slow ruptures was the widest for the ergosterol-containing GUVs (from less than 100 to approximately 500 μmol/l), narrower for the sterol-free GUVs (from 400 to 500 μmol/l) and the narrowest for the cholesterol-containing GUVs (only approximately 500 μmol/l) (Fig. 5). In addition, in the ergosterol-containing GUVs the concentration span was dependent on the ergosterol's molar fraction, i.e., larger values were found for the 15- and 45-mol% ergosterol-containing GUVs than for the 30-mol% ones.

Table 1
Dependence of the major characteristics of the fading process on the cholesterol content for the intermediate nystatin concentration range. The decrease rates of the fastest-fading phase and the final halo intensities are listed.

Cholesterol content [%]	Nystatin concentration [μmol/l]	Rate of halo intensity decrease [10^{-4} s^{-1}]	Final halo intensity [% of initial]
45	200	−0.7	76
0	200	−0.8	71
45	300	−3	13
45	400	−5	8
0	300	−13	12

4. Theoretical model

4.1. Basic overview

A theoretical model describing the characteristic patterns of vesicle behavior was developed. It is assumed that the observed behavior can be regarded as a consequence of an osmotic stress in the vesicles after the formation of the nystatin-induced transmembrane pores with a fixed diameter [43,49–51]. The transmembrane permeability, induced by these pores is size-discriminating [45] and, consequently, glucose molecules with a smaller effective radius experience a higher membrane permeability than the sucrose molecules [52]. Hence, the osmolarity of the solution inside the vesicle, which is initially equal to that of the glucose solution outside the vesicle, gradually increases after the formation of the nystatin pores. Consequently, an influx of water molecules into the vesicle is established, resulting in an increased volume of the vesicle, which induces an increased membrane tension and a corresponding hydrostatic pressure [49,51]. The phospholipid membrane water permeability is namely several orders of magnitude higher than the permeability of large sugar molecules [52,53]. This leads to a characteristic time for the water content and the osmotic pressure changes of approximately 0.2 s in a vesicle with a radius of 20 μm. On the other hand, the corresponding characteristic time for glucose molecules is approximately 2000 h.

In the next subsections the flow of water and sugar molecules through the nystatin transmembrane pores, and additionally, the flow of water directly through the intact phospholipid membrane, will be described. As a consequence of these flows, the increase in the vesicle volume and the membrane tension, followed by the incidence of a tension pore, will be presented in more detail.

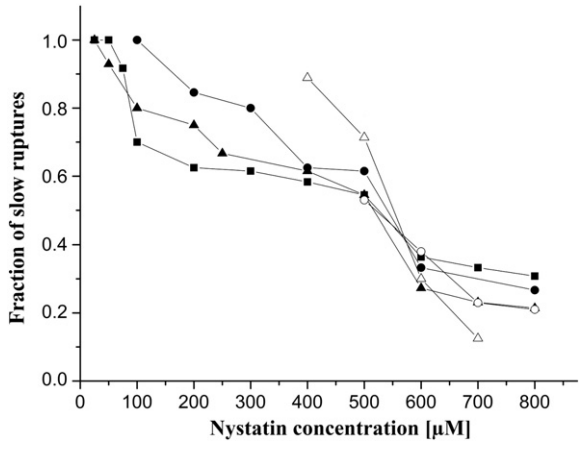

Fig. 5. Relationship between the relative fraction of slow ruptures with respect to the sum of slow ruptures and explosions, and the nystatin concentration at different vesicle compositions: sterol-free GUVs (Δ), and sterol-containing GUVs: 15 mol% (▲), 30 mol% (●), 45 mol% (■) ergosterol and 45 mol% cholesterol (○). The number of vesicles measured at each nystatin concentration was from 7 to 16 (11.3 ± 2.2). The lines between the measured points are drawn only to guide the eye.

4.2. Vesicle behavior before the formation of the tension pore

4.2.1. Flow through the nystatin pores

Both contributions of the volume flow, i.e., the flow of water, have to be considered: the flow directly through the phospholipid bilayer as well as the flow through the nystatin pores. In contrast, in the case of the solutes, i.e., sugar molecules, only the flow through the nystatin pores is relevant. In the model it was assumed that their number and radius do not change with time. The volume flow (J_{NP}) and the flow of the sugar molecules ($\Phi_{NP,i}$) through the nystatin pores depend on the difference in the hydrostatic pressures inside and outside the vesicle (Δp), and on the differences in the sugar number densities between the inner and outer solutions (Δc_i) [54], where i refers to glucose (G) or sucrose (S) molecules. The corresponding equations can be written as

$$J_{\mathrm{NP}} = -L_p(\Delta p - k_B T \textstyle\sum_i \sigma_i \Delta c_i) \tag{1}$$

for the volume flow, and

$$\Phi_{NP,i} = (1-\sigma_i)\bar{c}_i J_{NP} - P_i k_B T \Delta c_i \tag{2}$$

for the solute flow. The flows are taken to be positive when the volume of the vesicle increases and the number of sugar molecules in the vesicle increases. L_p is the hydraulic permeability for the pores, k_B is the Boltzmann constant, T is the absolute temperature, σ_i and $\bar{c}_i$ are the reflection coefficients and the mean solute concentrations, and P_i are the sugar permeabilities.

The sugar permeabilities (P_i) depend on the diffusion constant of each sugar molecule (D_i), the number and the radius of the peptide pores (N_P and R_{NP}), and the membrane thickness (d). If the nystatin pores are assumed to have a cylindrical shape and are equal in size, the permeabilities P_i can be described by the equation [55]:

$$P_i = D_i \frac{N_p \pi R_{NP}^2}{d} \times \left(1 - \frac{R_i}{R_{NP}}\right)^2 \times \left(1 - 2.104\frac{R_i}{R_{NP}} + 2.09\left(\frac{R_i}{R_{NP}}\right)^3 - 0.95\left(\frac{R_i}{R_{NP}}\right)^5\right), \tag{3}$$

with R_i being equal to the effective radii of the sugar molecules (R_S and R_G). It is clear that the membrane permeabilities depend on the ratio between R_i and R_{NP}.

4.2.2. Volume flow through the phospholipid bilayer

The volume flow through the phospholipid bilayer can be expressed in a similar way with the equation

$$J_{PB} = -A l_{PB}(\Delta p - k_B T \sum_i \Delta c_i), \tag{4}$$

where A is the membrane area and l_{PB} is the permeability coefficient of the phospholipid bilayer with respect to water.

4.2.3. Determination of the vesicle's volume and membrane tension

The volume of the vesicle is therefore determined by the sum of J_{NP} and J_{PB} [Eqs. (1) and (4)], which depend on the osmotic conditions, hence

$$\frac{dV}{dt} = J_{NP} + J_{PB}. \tag{5}$$

The osmotic pressure difference is given by the equation

$$\Delta\pi = k_B T\left(\frac{N_G}{V} - c_G + \frac{N_S}{V} - c_S\right), \tag{6}$$

where N_G and N_S denote the numbers of glucose and sucrose molecules in the vesicle with volume V, and c_G and c_S are the number densities of both sugars outside the vesicle. The latter two are taken to be constant, since the volume outside the vesicle is much larger than the vesicle volume, whereas the number of sugar molecules in the vesicle can be calculated using Eq. (2).

If the inflow of glucose molecules is larger than the outflow of sucrose molecules (the positive change in N_G is larger than the negative one in N_S), which is the case in our experiments, the volume of the vesicle and its membrane area increase. This affects the lateral tension (λ) in the vesicle membrane and, consequently, the hydrostatic pressure that can be expressed by the Laplace equation

$$\Delta p = \frac{2\lambda}{R_v}, \tag{7}$$

with R_v being the radius of the vesicle. The lateral tension in the membrane (λ) equals $k_A(A - A_0)/A_0$, where k_A is the membrane's expansivity modulus and A_0 is the membrane's equilibrium area.

4.3. Vesicle behavior after the formation of the tension pore

4.3.1. Incidence of the tension pore and the flow through it

When the membrane area reaches its critical value, corresponding to the critical membrane tension (λ_c) of the lipid bilayers [20,56,57], a tension pore occurs. The membrane area is decreased by the area of the tension pore if we assume that the radius of the vesicle remains constant during the formation of the tension pore. The mechanical energy of the vesicle (W) is determined by the sum of the membrane's stretching energy and the energy of the rim of the tension pore [50]. Taking into account the membrane undulations [58], the corresponding sum of the energy terms can be written in the form

$$W = \frac{k_A}{2A_0}\left(4\pi R_v^2 - A_L + \Delta A\left(1 - \frac{A_L}{4\pi R_v^2}\right) - A_0\right)^2 + \Gamma \times 2\pi r_{TP}, \tag{8}$$

where r_{TP} is the radius of the tension pore with the area equal to $A_L = 2\pi R_v\left(R_v - \sqrt{R_v^2 - r_{TP}^2}\right)$, and Γ is the line tension. ΔA is the total excess area due to the membrane undulations, that can be estimated by

$$\Delta A = A_0 \frac{k_B T}{8\pi k_c} \ln \frac{(R_v/d)^2 + \lambda R_v^2/k_c}{1 + \lambda R_v^2/k_c}, \tag{9}$$

with k_c the membrane bending constant [58] (Table 2).

The radius of the tension pore is determined by the minimum of W; therefore, at equilibrium the tension-pore radius as a function of k_A and Γ is determined by $\partial W/\partial r_{TP} = 0$. The pressure in the vesicle is larger than the pressure in the surroundings since the area of the membrane (A) is slightly larger than A_0 due to the membrane tension caused by the line tension. The membrane tension (λ) is calculated from the area of a slightly stretched vesicle membrane A, which is determined by the obtained radius of the tension pore r_{TP}. Using Eq. (7) the hydrostatic pressure difference can be expressed as

$$\Delta p = \frac{2\Gamma}{R_v r_{TP}(1 + \Delta A/A_0)}\sqrt{1 - \frac{r_{TP}^2}{R_v^2}}. \tag{10}$$

The tension pore offers an additional possibility for the passage of water and sugar molecules through the membrane. Consequently, a volume flow from the vesicle interior occurs through the tension pore. For $r_{TP} >> d$ this flow can be described by the equation for a plane with a circular opening [59]

$$J_{TP} = \frac{\Delta p r_{TP}^3}{3\eta}, \tag{11}$$

where η is the viscosity of the solution.

The solute flows of sugar molecules through the tension pore are proportional to the volume flow (J_{TP}). Thus, the corresponding flows of the sugar molecules through the tension pore are

$$\Phi_{TP,i} = \frac{N_i}{V} J_{TP}. \tag{12}$$

4.3.2. Total flow

When the tension pore is formed, the total volume flow is thus determined using Eqs. (1), (4) and (11)

$$\frac{dV}{dt} = J_{NP} + J_{PB} + J_{TP}, \tag{13}$$

whereas the total flow of sugar molecules is determined using Eqs. (2) and (12)

$$\frac{dN_i}{dt} = \Phi_{NP,i} + \Phi_{TP,i}. \tag{14}$$

It is assumed that the tension pore closes when the membrane's elastic energy of the vesicle with an open tension pore (W) is equal to the membrane's stretching energy of the vesicle with a closed tension pore. In the model we numerically solve Eqs. (13) and (14) in order to calculate the time dependence of the tension pore's radius and the vesicle's volume.

In accordance with the experiments, where the initial sucrose concentration inside the vesicle and the initial glucose concentration outside the vesicle were 0.2 mol/l, the corresponding initial number densities are taken to be $1.2 \times 10^{26}/m^3$. The initial number densities of the sucrose solution outside and the glucose solution inside the vesicle are zero. The radius of the vesicle is set to 20 μm and the membrane thickness to 5 nm. The glucose and sucrose hydrodynamic radii are taken to be equal to 0.36 nm and 0.46 nm [60], respectively, while the radius of the nystatin-induced pores is taken to be in the range from 0.4 to 1 nm. The diffusion constants for glucose and sucrose in water are 6.7×10^{-10} m^2/s and 5.2×10^{-10} m^2/s, respectively [53,61]. The viscosity of the solutions is taken to be 1×10^{-3} Pas and the absolute temperature, 297 K. The reflection coefficients for the glucose and sucrose molecules are determined in accordance with the experimental findings [62]: the coefficients are equal to 0.2 for $R_i/R_{NP} \leq 0.7$ and linearly increase as a function of R_i/R_{NP} from 0.2 to 1 at $0.7 < R_i/R_{NP} < 1$. The permeability coefficient of the phospholipid bilayer l_{PB} is equal to 4×10^{-13} m^3/(Ns) and the hydraulic permeability for the nystatin pores (L_p) is estimated with $N_P \times (\pi R_{NP}^4/(8\eta d))$, in accordance with the Hagen-Poisseuille law.

Table 2
Critical number of nystatin pores (N_P) during the transition from type-II to type-III tension-pore behavior for the POPC membrane without sterols and with the addition of 30 mol% ergosterol or 30 mol% cholesterol. They are calculated for the characteristic mechanical properties of the membrane: membrane's expansivity modulus (k_A), membrane's bending modulus (k_c), line tension (Γ) and lysis tension (λ_c) [20–22].

Sterol content [mol%]	k_A [J/m^2]	k_c [k_BT]	Γ [$\times 10^{-11}$ N]	λ_c [$\times 10^{-3}$ N/m]	N_P [$\times 10^7$]
0	0.213	38.5	2.6	7.8	5.7
30 (ergosterol)	0.241	54.6	2.9	9.5	6.8
30 (cholesterol)	0.354	86.8	3.41	11.9	7.0

4.4. Predictions of the model

4.4.1. Different types of tension-pore behavior

The model predicts three different vesicle responses in order to compensate for the net flow of water molecules into the vesicle due to the build-up of a higher concentration of sugar molecules inside the vesicle, which occurs as a consequence of the formation of the size-selective nystatin pores. For a small number of nystatin pores, only a short opening of the membrane occurs. A tension pore whose radius is a maximum at its occurrence is predicted. Its radius then decreases quickly until the tension pore closes (type-I tension-pore behavior, Fig. 6a). If the number of nystatin pores is increased, a long-lasting opening of the membrane is predicted (type-II tension-pore behavior, Fig. 6a). The radius of this type of tension pore also decreases quickly at the beginning; however, after a certain value is reached, the tension pore's radius starts to decrease significantly more slowly and the tension pore remains open for a longer period of time. For the largest numbers of nystatin pores a further increase in the tension pore's radius, which exceeds its initial value for the tension pore's occurrence, is theoretically predicted (type-III tension-pore behavior, Fig. 6a).

In all cases an increase in the volume (and the area) of the vesicle is predicted until the critical vesicle volume is reached. For low numbers of nystatin pores the water inflow, driven by the osmotic pressure, induces only a slowly increasing vesicle volume due to the sugar's low permeability of the nystatin pores. A short opening of the membrane (type-I tension pore) allows a quick and sufficient outflow of water and sucrose molecules, which is larger than the inflow. For the largest numbers of nystatin pores, in contrast, the occurrence of tension pore does not provide a sufficient volume outflow through the tension pore. Despite its large initial radius the outflow is still lower than the inflow as a result of the high sugar permeability of the nystatin pores and the volume of the vesicle increases further, above its critical value.

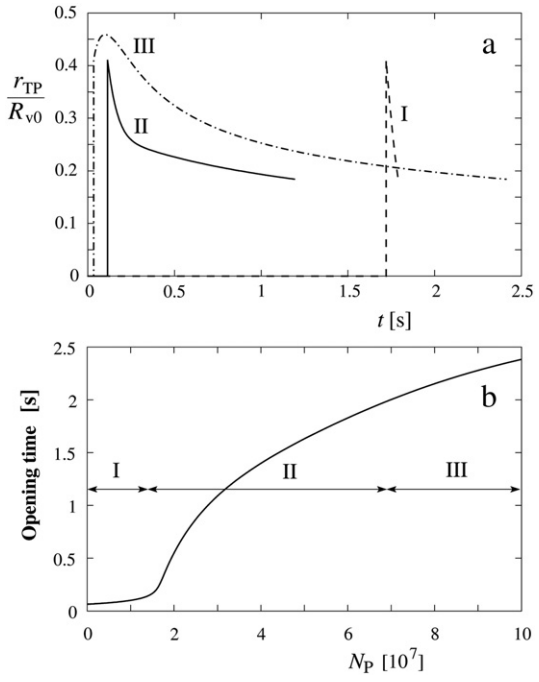

Fig. 6. Three characteristic types of tension-pore behavior predicted by the theory for a 0.45-nm nystatin pore radius in sterol-free vesicles. (a) An increase of the tension pore radius with respect to the initial vesicle radius (r_{TP}/R_{v0}), which could be assigned to type-I (dashed line), type-II (full line) and type-III (dash-dot line) tension-pore behavior, respectively. As an example, three different nystatin pore numbers representative for the type-I ($N_P = 5 \times 10^6$), for the type-II ($N_P = 3 \times 10^7$) and for the type-III ($N_P = 1 \times 10^8$) tension-pore behavior are depicted. (b) The opening time of the tension pores as a function of the number of nystatin pores. The ranges of different types of pore behavior (I, II and III) are also marked.

A further increase in the tension pore's radius over its initial value is needed to compensate for the net flow into the vesicle (type-III tension-pore behavior). For intermediate numbers of nystatin pores the sugar permeabilities and, consequently, the water inflow are somewhere in the middle. After the occurrence of tension pore an increase in the vesicle volume is prevented by the pore that lasts longer, but whose radius does not exceed its initial value (type-II tension-pore behavior). A rapid decrease of the tension pore's radius at the beginning is comparable to the type I; however, due to the higher inflow the tension pore cannot close quickly. In other words, the outflow through the tension pore significantly decreases with its radius and at a certain tension-pore radius the water outflow through the tension pore equilibrates the net inflow of water, which is higher for intermediate numbers of nystatin pores. Further changes in the tension-pore radius become much slower since the water inflow depends mainly on the sucrose concentration inside the vesicle, which slowly decreases.

The number of nystatin pores at which the type-I tension pore occurs is defined as the number of nystatin pores where at least one tension pore occurs within 60 minutes. The border between type-I and type-II tension-pore behavior is defined as the number of nystatin pores at which the opening time of the tension pore becomes twice as large and fits approximately to the maximum of the derivative of the duration of the tension pore's radius with respect to the pore number (Fig. 6b). It is characterized by the equilibration of the outflow through the tension pore with a net flow of water through the membrane at the minimum possible tension-pore radius (Section 4.3.2). The border between type-II and type-III tension-pore behavior is defined as the minimum number of nystatin pores at which the radius of the tension pore exceeds its initial value for the occurrence of tension pores. For a nystatin pore radius equal to 0.45 nm it is estimated that the number of nystatin pores for which the type-I tension pore occurs is equal to 1600 in a sterol-free membrane. For the transition from type-I to type-II tension-pore behavior the predicted nystatin pore number is equal to 1.3×10^7. Furthermore, for the occurrence of the type-III tension-pore behavior the nystatin pore number should exceed 6.9×10^7.

4.4.2. Influences of the membrane's mechanical characteristics on the behavior of the tension pore

The experimentally determined changes in the membrane's mechanical properties for the sterol-free POPC membrane after the addition of 30% ergosterol and 30% cholesterol are listed in Table 2. In order to simulate the influences of the changed membrane's expansivity modulus (k_A), line tension (Γ) and lysis tension (λ_c), let us concentrate on the changes in the number of nystatin pores needed for the transition from type-II to type-III tension-pore behavior. Using a 0.45-nm nystatin pore radius the model predicts a net increase of 13% for the ergosterol-containing and 11% for cholesterol-containing membranes in comparison to a sterol-free membrane. The model also

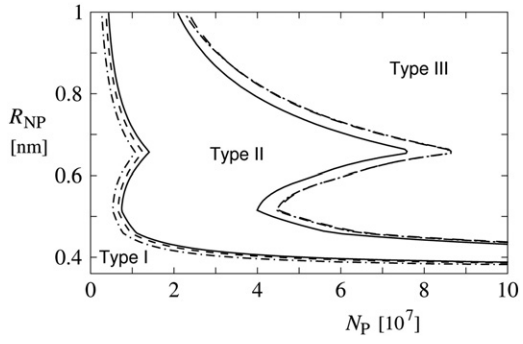

Fig. 7. Three characteristic types of tension-pore behavior as a function of the number and the radius of the nystatin pores (N_P and R_{NP}). Note the minor influence of the changed mechanical parameters of the membrane for the sterol-containing membrane with the addition of 30 mol% ergosterol (dashed line) or 30 mol% cholesterol (dash-dot line) in comparison with the sterol-free membrane (full line).

offers the possibility to study the changes in the tension pore's behavior if the individual parameter changes are considered. All of them are higher in the cholesterol-containing membrane than in the ergosterol-containing membrane.

The effects due to different mechanical characteristics of the membrane can be presented in a more general case. In Fig. 7 the regions of different tension-pore behavior are shown in the form of a phase diagram as a function of the nystatin pore's radius and the pore number. It can be seen that the same types of tension-pore behavior are mainly met for a smaller number of nystatin pores if the radius of the pore is increased. Furthermore, the borders between types I and II tension-pore behavior are shifted in the cholesterol- and ergosterol-containing membranes towards smaller numbers of nystatin pores. These shifts are more pronounced in the cholesterol-containing membrane. The borders between type II and III tension-pore behavior are shifted towards larger numbers of nystatin pores by comparable values in both sterol-containing membranes.

4.5. Limitations of the model

It is important to point out some limitations of the model. It is assumed that the glucose and sucrose molecules do not disturb each other in their passage through the nystatin pore. In addition, it is assumed that the nystatin membrane's incorporation and/or the pore formation do not change the mechanical properties of the membrane. For a vesicle with a radius equal to 20 μm the formation of 1×10^7 nystatin pores with a radius of 0.45 nm would represent only 0.13 % of the total vesicle membrane area, which supports the basis of this assumption. Furthermore, it should be noted that no temporal evolution of the number and/or the radius of the nystatin pores has been incorporated into the theoretical model. Nevertheless, our primary goal, i.e., a basic understanding of the distinct differences in the behavior patterns of the vesicles, could be achieved.

5. Discussion

Although the discovery and the use of different antibiotics changed the treatment and the outcome of infections dramatically, the mode of action of certain antibiotic classes remains to be completely understood. Studies of the influence of the polyene nystatin on giant unilamellar vesicles using phase-contrast microscopy offer a chance to visualize the membrane effects induced by this antibiotic on the level of individual vesicles with dimensions that are relevant for an average human cell. The investigations of sterol-free POPC GUVs revealed a variety of effects, i.e., vesicle shape changes, the formation of transient tension pores and the total destruction of the vesicle [43]. Hence, a straightforward question occurs regarding the influence of membrane sterols on the phenomena described.

5.1. Interpretation of the theoretical predictions

A theoretical model based on the theory of osmotic lysis [50] and the pore-diffusion theory [55] was developed in order to understand the experimental results (supplementary video material – Appendix B). Three distinctly different types of tension-pore behavior can be theoretically predicted (Fig. 6a). A close resemblance to the experimentally observed vesicle behavior patterns, i.e., membrane bursts, slow vesicle ruptures and explosions (Figs. 1c, 3 and 6), is identified. Membrane bursts can be correlated with type-I tension pores (Figs. 1c and 6a). The observed slow ruptures can be recognized as type-II tension pores (Figs. 3a and 6a) and vesicle explosions as theoretically predicted type-III tension pores (Figs. 3b and 6a). For a better match with the experimental observations, however, it should be kept in mind that some of the observed slow ruptures do not close as predicted by the theoretical model, presumably due to the potential instabilities of open surfaces [63], a process that is not included in our model. Nevertheless, a good correlation between the types of tension pores predicted by the theoretical model and the experimentally observed behavior of the vesicles confirms the importance of the osmotic phenomena and the restricted pore diffusion in the action of nystatin and similar pore-forming agents on the phospholipid membrane.

5.2. Effects of ergosterol and cholesterol on the nystatin membrane activity

5.2.1. Basic features

The experimental results show that the succession of the characteristic vesicle behavior patterns, i.e., morphological alterations → membrane bursts → slow vesicle ruptures → explosions, are preserved with an increasing nystatin concentration. In accordance with the literature [32, 33,40], the cholesterol shifts the typical vesicle responses to a minor extent towards higher nystatin concentrations, while the addition of ergosterol shifts these responses drastically towards lower nystatin concentrations, compared to the sterol-free membrane. Most strikingly, the slow vesicle ruptures start significantly sooner, i.e., at 4–5 times lower nystatin concentrations, in the ergosterol-containing vesicles (Fig. 5). The early occurrence of slow ruptures in the ergosterol-containing membranes might play, in addition to the disruption of the transmembrane electrochemical gradients, an important role in the medical treatment of fungal diseases with nystatin.

5.2.2. Role of the altered membrane's mechanical characteristics

The addition of cholesterol and ergosterol changes the membrane's mechanical properties (Table 2); however, the impact of these sterol specific influences on the nystatin activity has not yet been fully quantitatively characterized [17–22]. Based on the presented theoretical model, a more precise delineation of the role of the changed mechanical properties of the membrane is obtained. The predictions of the model show that an increase in the membrane's expansivity modulus (k_A) and the membrane's bending modulus (k_c) has the opposite effect to an increase in the line tension (Γ) and the lysis tension (λ_c). All these antagonizing sterol-induced changes to the membrane's mechanical properties can be compensated for by a maximum change in the number of nystatin pores of only approximately 30% in the 30-mol% ergosterol- and cholesterol-containing membranes in order to obtain the same vesicle response as in the sterol-free membranes. The model predicts a comparable 13% net compensatory change of nystatin pores in a 45-mol% cholesterol-containing membrane. Hence, the small extent of these changes clearly shows that the significantly different behavior of the ergosterol-containing vesicles cannot be adequately explained by the changes in the membrane's mechanical characteristics.

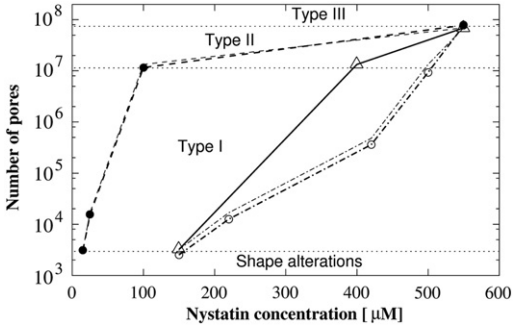

Fig. 8. Schematic dependence of the number of nystatin pores on the nystatin concentration in the solution surrounding the vesicle for sterol-free (Δ, full line), 30-mol% cholesterol- (○, dash-dot line) and for 30-mol% ergosterol-containing membrane (●, dashed line). The thinner lines denote the sterol-containing membranes before the modulation due to the changed mechanical characteristics of the membrane. The thin dotted lines divide the areas where the shape alterations, type-I, type-II and type-III tension-pore behavior occur.

5.2.3. Changes in vesicle behavior due to altered nystatin membrane binding, partition and aggregation

Since the experimental results cannot be explained on the basis of the changed mechanical characteristics, the primary focus should be placed on nystatin binding, partitioning and its aggregation in the membrane and, consequently, on the formation of the nystatin pores. A schematic diagram that shows the dependence of the number of nystatin pores on its concentration in the surrounding medium is presented in Fig. 8. It is obtained from the correlation of the predictions of the theoretical model and the experimental observations (Appendix A).

The curves obtained in Fig. 8 clearly demonstrate that the ergosterol curve is distinctly different from the cholesterol and the sterol-free curves and can serve as a theoretical illustration of the experimentally determined distinctions between the responses of the sterol-containing and sterol-free vesicles. In the ergosterol-containing membranes, a significantly quicker formation of nystatin pores is seen at lower nystatin concentrations (below 100 μmol/l), while a slower increase in the number of nystatin pores is observed at higher concentrations. In contrast to this, a slower increase in the number of nystatin pores at lower nystatin concentrations and a faster increase at higher concentrations are induced in the cholesterol-containing and the sterol-free membranes (Fig. 8). This can be associated with a more efficient decrease of the halo intensity and an earlier occurrence of the slow ruptures in the ergosterol-containing vesicles and, vice versa, a less efficient decrease of the halo intensity, a shift of the occurrence of slow ruptures to higher nystatin concentrations and a transition from slow ruptures to explosions at a smaller nystatin concentration span in the cholesterol-containing and the sterol-free membranes. The obtained schematic dependencies of the sterol-free and the sterol-containing GUVs exposed to different nystatin concentrations are in accordance with the fact that cholesterol inhibits the effects of nystatin, while ergosterol, despite being only slightly structurally different, facilitates them [32,33,40]. They also support the findings that nystatin can form pores in the sterol-free membranes [29,42,43] and demonstrate comparable effects in sterol-free and cholesterol-containing membranes. Furthermore, our experimental and theoretical results are in accordance with the significantly higher time average conductance [64] as well as higher % K^+ dissipation and the apparent initial rate of the pore formation [41] reported in the ergosterol-containing vesicles in comparison with the cholesterol-containing ones. The latter were accompanied by the changes in the fluorescence lifetime of the nystatin molecules due to the formation of nystatin-nystatin or nystatin-sterol complexes in the lipid membranes [41].

5.3. Effects of variations in the membrane ergosterol content on the nystatin membrane activity

The measurements confirmed that the ergosterol molar fraction is a very important parameter affecting the nystatin activity in the ergosterol-POPC membrane. The greatest effects of nystatin, i.e., the vesicle halo-intensity decrease and the vesicle ruptures, were detected at 45%, the intermediate at 15% and the lowest ones at 30% ergosterol membrane molar fraction (Figs. 2, 4 and 5). A 15% change in the ergosterol membrane molar content is, for example, more important than a nystatin concentration increase from 25 to 100 μmol at a 30% ergosterol molar fraction. This molar change induces slow vesicle ruptures at a 25-μmol/l nystatin concentration for 15% and 45% ergosterol molar fractions, while they occur for the first time at a 100-μmol/l nystatin concentration for a 30% ergosterol molar fraction (Figs. 2 and 5). The observed effects cannot be explained by the influences of ergosterol molar fractions on the basis of the changed mechanical characteristics of the membrane. The addition of ergosterol into the membranes results in an increase of the membrane's mechanical parameters nearly in proportion to the increasing ergosterol molar fraction [20–22]. In addition, the maximal nystatin pore number changes of approximately 20% are predicted by the theoretical model to obtain a comparable tension-pore behavior if the changes in the experimentally determined values for k_A, k_c, Γ and λ_c in the POPC membranes with 15%, 30% and 45% mol% ergosterol are considered.

Therefore, the sterol-induced changes in the membrane's structural properties, such as the regularity of the membrane lipid organization, and their effects on the pore formation process should again be primarily considered. Our experimental results (Fig. 5) agree on a qualitative level with the predictions of the superlattice sterol lateral organization models. These models predict that the nystatin membrane partition is decreasing in a similar manner: 45 mol% (major local maximum) → 15 mol% (minor local maximum) → 30 mol% (local minimum), in accordance with the extent of the sterol regular distribution regions [10,24,25].

Alternatively, the POPC-sterol phase diagrams demonstrate a progressive predominance of a liquid-ordered phase with an increasing sterol membrane content from the liquid-disordered (ld) over the co-existence of liquid-disordered and liquid-ordered phase (ld + lo) to a single liquid-ordered (lo) phase [41]. Thus, a diminishment of nystatin effects with increasing sterol content is expected if the ordering of membranes hinders the partition and the formation of nystatin pores. Nevertheless, our experiments with ergosterol show a minimal nystatin activity in the middle of the ld + lo phase. This implies that either a more complex membrane behavior of POPC/ergosterol binary mixture [39] or a more complex dependency of nystatin activity on the regularity of the membrane's lipid organization exists [65].

6. Conclusions

The effects of ergosterol and cholesterol on the nystatin membrane activity were studied in GUVs using phase-contrast microscopy. The experimental results were compared to the characteristic vesicle behavior observed in the sterol-free vesicles and correlated with the theoretical model.

The experimental results demonstrated more intense effects in the ergosterol-containing membranes. Membrane bursts, slow ruptures and vesicle explosions were detected at significantly lower nystatin concentrations than for the sterol-free and cholesterol-containing membranes. In addition, an early beginning and a significant prolongation of the nystatin concentration span, characterized by the slow vesicle ruptures, could be observed in the ergosterol-containing membranes, which might be an important mechanism leading to cell death in ergosterol-containing fungal cells.

A theoretical model based on restricted pore diffusion and the theory of osmotic lysis predicts three different types of tension-pore behavior, depending on the number of nystatin pores. The observed experimental results can primarily be explained by a significantly higher membrane-binding and pore-formation rate at lower nystatin concentrations in the ergosterol-containing vesicles in comparison with the cholesterol-containing and sterol-free vesicles. The role of the changed mechanical characteristics of the membrane, i.e., the membrane's expansivity modulus, line tension and lysis tension, which could be quantitatively differentiated from the nystatin pore formation activity, was found to be of secondary importance for the explanation of the observed differences in the vesicle behavior. In addition, the role of ergosterol membrane molar fraction was found to be crucial, especially due to its nonlinear effects.

In conclusion, the changes in the phospholipid vesicle behavior induced by different membrane sterol contents were observed and a basic understanding of this behavior could be achieved. Although a more quantitative comparison to the experimental data is still lacking, these results should be regarded as a step towards a more profound understanding of the action of polyene antibiotics in biological membranes.

Acknowledgements

We would like to thank S. Svetina for fruitful discussions and valuable suggestions, and V. Arrigler, A. Cimprič and U. Klančnik for

their help in the laboratory and the preparations of the phospholipid vesicles. This work was financially supported by the Slovenian Research Agency grant P1-0055.

Appendix A. Correlation between the theoretical predictions and the experimental observations

The dependence of the number of nystatin pores on its concentration in the surrounding medium, presented in Fig. 8, is obtained from the correlation of the following theoretical and experimental results:

i) A sufficient number of nystatin pores for the bursts (type-I tension pores) that are observed at approximately a 10–20 μmol/l nystatin concentration in ergosterol-containing membranes and at approximately 100–200 μmol/l in the cholesterol-containing and the sterol-free vesicles (Figs. 2 and 4) is equal to 1.6×10^3, according to the theoretical predictions. This number of nystatin pores was multiplied by 2, since significant halo-intensity changes can be detected experimentally when at least two consecutive bursts occur.

ii) Slow ruptures (type-II tension pores) that are theoretically predicted above 1.3×10^7 nystatin pores are observed at a 100-μmol/l nystatin concentration in ergosterol-containing vesicles, which is a significantly lower than the 500 μmol/l and 400 μmol/l in cholesterol-containing and sterol-free vesicles (Figs. 4 and 5).

iii) The nystatin concentration at which the explosions (type-III tension pores) become more frequent than the slow ruptures was found to be, regardless of the membrane composition, approximately 550 μmol/l (Fig. 5). This implicates roughly the same theoretically determined number of nystatin pores (6.9×10^7 nystatin pores) associated with the transition from type-II to type-III tension-pore behavior. It may seem to be an oversimplification, because in the ergosterol-containing membranes the transition is much more gradual, but nevertheless, the point where the explosions prevail may be determined in spite of this.

iv) The slope of the halo-intensity decrease is approximately the same at a 25-μmol/l nystatin concentration in ergosterol-containing vesicles compared to approximately 200 μmol/l and 220 μmol/l in the sterol-free and in the cholesterol-containing vesicles, which also implies the same number of nystatin pores at these concentrations (Figs. 2 and 4).

v) The halo-intensity decrease in the cholesterol-containing vesicles is slightly lower at the 400-μmol/l nystatin concentration compared to that of the sterol-free ones at 300 μmol/l (Fig. 4), which implies a comparable number of nystatin pores at these two concentrations.

At the end, the obtained curves for the ergosterol- and cholesterol-containing vesicles in Fig. 8 were corrected in order to compensate for the sterol-induced changes of the membrane's mechanical parameters.

Appendix B. Supplementary data

Supplementary video material presenting three distinctly different types of the observed tension-pore behavior can be found online. An example of membrane bursts can be found in supplementary data to Ref. [43]. Supplementary video material to this article contains examples of two types of slow vesicle ruptures. The first slow rupture demonstrates a large membrane opening, which reseals afterwards, while the second one represents a more seldom encountered stable opening with a distinctive orifice leading to a vesicle disintegration into an amorphous lipid debris. Supplementary video material to this article also contains an example of a vesicle explosion. Supplementary data to this article can be found online at http://dx.doi.org/10.1016/j.bbamem.2014.05.019.

References

[1] E.M. Johnson, J.O. Ojwang, A. Szekely, T.L. Wallace, D.W. Warnock, Comparison of in vitro antifungal activities of free and liposome-encapsulated nystatin with those of four amphotericin B formulations, Antimicrob. Agents Chemother., 42, 1998, pp. 1412–1416.
[2] C.P. Schaffner, Polyene macrolides in clinical practice: pharmacology and other adverse effects, in: S. Omura (Ed.), Macrolide antibiotics: Chemistry, biology and practice, second ed., Academic Press, New York, 2002, pp. 457–507.
[3] J. Bolard, How do the polyene macrolide antibiotics affect the cellular membrane properties? Biochim. Biophys. Acta 864 (1986) 257–304.
[4] S.C. Hartsel, C. Hatch, W. Ayenew, How does amphotericin B work? Studies on model membrane systems, J. Liposome Res. 3 (1993) 377–408.
[5] A. Coutinho, M. Prieto, Cooperative partition model of nystatin interaction with phospholipid vesicles, Biophys. J. 84 (2003) 3061–3078.
[6] R. Holz, A. Finkelstein, The water and nonelectrolyte permeability induced in thin lipid membranes by the polyene antibiotics nystatin and amphotericin B, J. Gen. Physiol. 56 (1970) 125–145.
[7] R.L. Hoover, E.A. Dawidowicz, J.M. Robinson, M.J. Karnovsky, Role of cholesterol in the capping of surface immunoglobulin receptors on murine lymphocytes, J. Cell Biol. 97 (1983) 73–80.
[8] F. Liu, P.L.-G. Chong, Evidence for a regulatory role of cholesterol superlattices in the hydrolitic activity of secretory phospholipase A2 in lipid membranes, Biochemistry 38 (1999) 3867–3873.
[9] M.M. Wang, M. Olsher, I.P. Sugar, P.L.-G. Chong, Cholesterol superlattice modulates the activity of cholesterol oxidase in lipid membranes, Biochemistry 43 (2004) 2159–2166.
[10] M.M. Wang, I.P. Sugar, P.L.-G. Chong, Role of the sterol superlattice in the partitioning of the antifungal drug nystatin into lipid membranes, Biochemistry 37 (1998) 11797–11805.
[11] D.A. Brown, E. London, Functions of lipid rafts in biological membranes, Annu. Rev. Cell Dev. Biol. 14 (1998) 111–136.
[12] A. Radhakrishnan, H.M. McConnell, Condensed complexes of cholesterol and phospholipids, Biophys. J. 77 (1999) 1507–1517.
[13] J. Henriksen, A.C. Rowat, E. Brief, Y.W. Hsueh, J.L. Thewalt, M.J. Zuckermann, J.H. Ipsen, Universal behavior of membranes with sterols, Biophys. J. 90 (2006) 1639–1649.
[14] E. Karatekin, O. Sandre, H. Guitouni, N. Borghi, P.-H. Puech, F. Brochard-Wyart, Cascade of transient pores in giant vesicles: line tension and transport, Biophys. J. 84 (2003) 1734–1749.
[15] T. Portet, R. Dimova, A new method for measuring edge tensions and stability of lipid bilayers: effect of membrane composition, Biophys. J. 99 (2010) 3264–3273.
[16] E. Evans, W. Rawicz, Entropy-driven tension and bending elasticity in condensed-fluid membranes, Phys. Rev. Lett. 64 (1990) 2094–2097.
[17] G. Orädd, V. Shahedi, G. Lindblom, Effect of sterol structure on the bending rigidity of lipid membranes: A ^{2}H NMR transverse relaxation study, Biochim. Biophys. Acta 1788 (2009) 1762–1771.
[18] H.P. Duwe, J. Kaes, E. Sackmann, Bending elastic-moduli of lipid bilayers – modulation by solutes, J. Phys. 51 (1990) 945–962.
[19] P. Meleard, C. Gerbeaud, T. Pott, L. Fernandez Puente, I. Bivas, M.D. Mitov, J. Dufourcq, P. Bothorel, Bending elasticities of model membranes: Influences of temperature and sterol content, Biophys. J. 72 (1997) 2616–2629.
[20] Y.W. Hsueh, M.T. Chen, P.J. Patty, C. Code, J. Cheng, B.J. Frisken, M. Zuckermann, J. Thewalt, Ergosterol in POPC membranes: Physical properties and comparison with structurally similar sterols, Biophys. J. 92 (2007) 1606–1615.
[21] J. Henriksen, A.C. Rowat, J.H. Ipsen, Vesicle fluctuation analysis of the effects of sterols on membrane bending rigidity, Eur. Biophys. J. 33 (2004) 732–741.
[22] K.J. Tierney, D.E. Block, M.L. Longo, Elasticity and phase behavior of DPPC membrane modulated by cholesterol, ergosterol, and ethanol, Biophys. J. 89 (2005) 2481–2493.
[23] A. Radhakrishnan, H.M. McConnell, Condensed complexes in vesicles containing cholesterol and phospholipids, Proc. Natl. Acad. Sci. U. S. A. 102 (2005) 12662–12666.
[24] P.L.-G. Chong, Evidence for regular distribution of sterols in liquid crystalline phosphatidylcholine bilayers, Proc. Natl. Acad. Sci. 91 (1994) 10069–10073.
[25] P.L.-G. Chong, W. Zhu, B. Venegas, On the lateral structure of model membranes containing cholesterol, Biochim. Biophys. Acta 1788 (2009) 2–11.
[26] D. Tang, P.L.-G. Chong, E/M dips: evidence for lipids regularly distributed into hexagonal super-lattices in pyrene-PC/DMPC binary mixtures at specific concentrations, Biophys. J. 63 (1992) 903–910.
[27] I.P. Sugar, D. Tang, P.L.-G. Chong, Monte Carlo simulation of lateral distribution of molecules in a two-component lipid membrane. Effect of long-range repulsive interactions, J. Phys. Chem. 98 (1994) 7201–7210.
[28] P.L.-G. Chong, D. Tang, I.P. Sugar, Exploration of physical principles underlying lipid regular distribution: effects of pressure, temperature, and radius of curvature on E/M dips in pyrene-labeled PC/DMPC binary mixtures, Biophys. J. 66 (1994) 2029–2038.
[29] K. Hąc-Wydro, J. Kapusta, A. Jagoda, P. Wydro, P. Dynarowicz-Łątka, The influence of phospholipid structure on the interactions with nystatin, a polyene antifungal antibiotic, A langmuir monolayer study, Chem. Phys. Lipids 150 (2007) 125–135.
[30] A. Coutinho, L. Silva, A. Fedorov, M. Prieto, Cholesterol and ergosterol influence nystatin surface aggregation: relation to pore formation, Biophys. J. 87 (2004) 3264–3276.
[31] L. Silva, A. Coutinho, A. Fedorov, M. Prieto, Nystatin-induced lipid vesicle permeabilization is strongly dependent on sterol structure, Biochim. Biophys. Acta 1758 (2006) 452–459.

[32] B. de Kruijff, W.J. Gerritsen, R.A. Demel, Polyene antibiotic-sterol interactions in membranes of *Acholeplasma laidlawii* cells and lecithin liposomes, III. Molecular structure of the polyene antibiotic-cholesterol complexes, Biochim. Biophys. Acta 339 (1974) 57–70.
[33] P. van Hoogevest, B. de Kruijff, Effect of amphotericin B on cholesterol-containing liposomes of egg phosphatidylcholine and didocoseneoylphosphatidylcholine, A refinement of the model for the formation of pores by amphotericin B in membranes, Biochim. Biophys. Acta 511 (1978) 397–407.
[34] C.C. Hsu Chen, D.S. Feingold, Polyene antibiotic action on lecithin liposomes: Effect of cholesterol and fatty acyl chains, Biochem. Biophys. Res. Commun. 51 (1973) 972–978.
[35] A. Marty, A. Finkelstein, Pores formed in lipid bilayer membranes by nystatin, differences in its one-sided and two-sided action, J. Gen. Physiol. 65 (1975) 515–526.
[36] J. Czub, M. Baginski, Comparative molecular dynamics study of lipid membranes containing cholesterol and ergosterol, Biophys. J. 90 (2006) 2368–2382.
[37] E. Endress, S. Bayerl, K. Prechtel, C. Maier, R. Merkel, T.M. Bayerl, The effect of cholesterol, lanosterol, and ergosterol on lecithin bilayer mechanical properties at molecular and microscopic dimensions: a solid-state NMR and micropipet study, Langmuir 18 (2002) 3293–3299.
[38] Y.W. Hsueh, K. Gilbert, C. Trandum, M. Zuckermann, J. Thewalt, The effect of ergosterol on dipalmitoylphosphatidylcholine bilayers: a deuterium NMR and calorimetric study, Biophys. J. 88 (2005) 1799–1808.
[39] J.A. Urbina, S. Pekerar, H. Le, J. Patterson, B. Montez, E. Oldfield, Molecular order and dynamics of phosphatidylcholine bilayer membranes in the presence of cholesterol, ergosterol and lanosterol: a comparative study using ^{2}H-, ^{13}C- and ^{31}P-NMR spectros, Biochim. Biophys. Acta 1238 (1995) 163–176.
[40] J. Gabrielska, M. Gagos, J. Gubernator, W.I. Gruszecki, Binding of antibiotic amphotericin B to lipid membranes: A ^{1}H NMR study, FEBS Lett. 580 (2006) 2677–2685.
[41] L. Silva, A. Coutinho, A. Fedorov, M. Prieto, Competitive binding of cholesterol and ergosterol to the polyene antibiotic nystatin. A fluorescence study, Biophys. J. 90 (2006) 3625–3631.
[42] K. Hąc-Wydro, P. Dynarowicz-Łątka, Interaction between nystatin and natural membrane lipids in Langmuir monolayers - The role of a phospholipid in the mechanism of polyenes mode of action, Biophys. Chem. 123 (2006) 154–161.
[43] L. Kristanc, S. Svetina, G. Gomišček, Effects of the pore-forming agent nystatin on giant phospholipid vesicles, Biochim. Biophys. Acta 1818 (2012) 636–644.
[44] M. Moreno-Bello, M. Bonilla-Marín, C. González-Beltrán, Distribution of pore sizes in black lipid membranes treated with nystatin, Biochim. Biophys. Acta 944 (1988) 97–100.
[45] M.E. Kleinberg, A. Finkelstein, Single-length and double-length channels formed by nystatin in lipid bilayer membranes, J. Membr. Biol. 80 (1984) 257–269.
[46] A.K. Solomon, C.M. Gary-Bobo, Aqueous pores in lipid bilayers and red cell membranes, Biochim. Biophys. Acta 255 (1972) 1019–1021.
[47] T. Katsu, S. Okada, T. Imamura, K. Komagoe, K. Masuda, T. Inoue, S. Nakao, Precise size determination of amphotericin B and nystatin channels formed in erythrocyte and liposomal membranes based on osmotic protection experiments, Anal. Sci. 24 (2008) 1551–1556.
[48] M.I. Angelova, S. Soleau, P. Meleard, F. Faucon, P. Bothorel, Preparation of giant vesicles by external AC electric fields: kinetics and applications, Progr. Colloid Polym. Sci. 89 (1992) 127–131.
[49] M. Mally, J. Majhenc, S. Svetina, B. Žekš, Mechanisms of equinatoxin II-induced transport through the membrane of a giant phospholipid vesicle, Biophys. J. 83 (2002) 944–953.
[50] M.M. Koslov, V.S. Markin, A theory of osmotic lysis of lipid vesicles, J. Theor. Biol. 109 (1984) 17–39.
[51] M. Mally, J. Majhenc, S. Svetina, B. Žekš, The response of giant phospholipid vesicles to pore-forming peptide melittin, Biochim. Biophys. Acta 1768 (2007) 1179–1189.
[52] R.E. Wood, F.P. Wirth Jr., H.E. Morgan, Glucose permeability of lipid bilayer membranes, Biochim. Biophys. Acta 163 (1968) 171–178.
[53] D. Huster, A.J. Jin, K. Arnold, K. Gawrisch, Water permeability of polyunsaturated lipid membranes measured by 17O NMR, Biophys. J. 73 (1997) 855–864.
[54] A. Katchalsky, P.F. Curran, Nonequilibrium thermodynamics in biophysics, Harvard University Press, Cambridge, Mass, 1965.
[55] E.M. Renkin, Filtration, diffusion and molecular sieving through porous cellulose membranes, J. Gen. Physiol. 38 (1954) 225–243.
[56] M. Bloom, E. Evans, O.G. Mouritsen, Physical properties of the fluid-bilayer component of cell membranes: a perspective, Q. Rev. Biophys. 24 (1991) 293–397.
[57] E. Evans, V. Heinrich, F. Ludwig, W. Rawicz, Dynamic tension spectroscopy and strength of biomembranes, Biophys. J. 85 (2003) 2342–2350.
[58] E. Evans, W. Rawicz, B.A. Smith, Concluding remarks, back to the future: mechanics and thermodynamics of lipid biomembranes, Faraday Discuss. 161 (2013) 591–611.
[59] J. Happel, H. Brenner, in: M. Nijhoff (Ed.), In axisymmetrical flow in low Reynolds number hydrodinamics, Kluwer, The Hague, The Netherlands, 1983, pp. 97–158.
[60] R. Scherrer, P. Gerhardt, Molecular sieving by the *Bacillus megaterium* cell wall and protoplast, J. Bacteriol. 107 (1971) 718–735.
[61] D.R. Lide (Ed.), CRC handbook of chemistry and physics, CRC Press, Boca Raton, FL, 2005.
[62] J.S. Schultz, R. Valentine, C.Y. Choi, Reflection coefficients of homopore membranes: effect of molecular size and configuration, J. Gen. Physiol. 73 (1979) 49–60.
[63] R. Capovilla, J. Guven, J.A. Santiago, Lipid membranes with an edge, Phys. Rev. E 66 (2002) 021607-1–021607-7.
[64] K.S. Récamier, A. Hernández-Gómez, J. González-Damián, I. Ortega-Blake, Effect of membrane structure on the action of polyenes: I. Nystatin action in cholesterol- and ergosterol-containing membranes, J. Membr. Biol. 237 (2010) 31–40.
[65] J. González-Damián, I. Ortega-Blake, Effect of membrane structure on the action of polyenes II: nystatin activity along the phase diagram of ergosterol- and cholesterol-containing POPC membranes, J. Membr. Biol. 237 (2010) 41–49.